

Fibre Bridging and Crack Tip Shielding in Glare: Numerical and Experimental Validation

Sunil Bhat¹

¹ School of Mechanical and Building Sciences, VIT Univeristy, Vellore, 632014, Tamil Nadu, India

* Corresponding author: ss_bht @rediffmail.com

Abstract The paper validates the phenomenon of fibre bridging and crack tip shielding in Fibre Metal Laminate (Glare) with the help of numerical and experimental procedures. Laminates, with Mode I cracks of different sizes in all their aluminum layers, are subjected to load-extension test to obtain critical loads for estimation of their fracture toughness. Similarly cracked, plain aerospace aluminum alloy specimens are also tested for fracture. Fracture toughness of Glare laminates is found to be higher than those of plain aluminum alloy specimens. Cracked laminates are finally modeled under critical loads by finite element method for quantification of fibre bridging in them. Crack tip shielding is demonstrated.

Keywords Fibre metal laminate, Fibre bridging, Glare, Crack tip shielding

1. Introduction

Fibre metal laminate (FML) is an advanced hybrid structure that consists of layers of thin and light metallic sheets which are alternately bonded and cured with composite prepregs by heat and pressure, each prepreg built up of several resin impregnated fibre cloth layers laid in similar or different orientations. Besides offering gain in specific strength, FML exhibits properties like excellent fatigue and fracture resistance, good impact strength and high fire resistance that makes it a good substitute for monolithic metallic structure especially in aerospace and aircraft applications. FML (Glare), comprising several aerospace aluminum alloy layers and glass fibre based composite prepregs, is considered for investigation in the present work.

Cracks can nucleate in soft aluminum layers, across the interfaces of prepregs, when Glare is pressed into service. The cracks are however shielded due to fibre bridging. Bridging diverts load towards stronger fibres in prepregs that in turn diminishes the intensity of stress fields around crack tips thereby augmenting fracture toughness of Glare vis-à-vis plain aerospace aluminum alloy. Published work, notably by Guo *et al.* [1], Alderliesten *et al.* [2] etc., confirms superior fatigue and fracture properties of FML's. This paper presents an explicit validation of the phenomenon of fibre bridging in Glare with the help of numerical and experimental procedures. Glare laminates, with Mode I cracks of different sizes in all their aluminum layers, are subjected to load-extension test to obtain break or critical loads for estimation of their fracture toughness. Similarly cracked, plain aerospace aluminum alloy specimens are also tested for fracture. Toughness values of laminates are found to be higher than that of plain aluminum alloy specimens. The laminates are finally modeled under critical loads by finite element method. Crack tip shielding in them is demonstrated and convincingly verified.

2. Construction of Glare

Refer Figure 1. Glare laminate consists of three, 0.4 mm thick, 2014-T6 aerospace aluminum alloy sheets, bonded alternately with two prepregs at curing temperature of 160 deg. C, each prepreg built up of three composite layers in the sequence, c0-c90-c0. A composite layer consists of 4 mil or 0.1mm thick unidirectional E-glass fibre cloth that is coated on both the sides with a thin layer of epoxy resin. Composite, c0, has fibres laid in y direction i.e. along the direction of the applied load

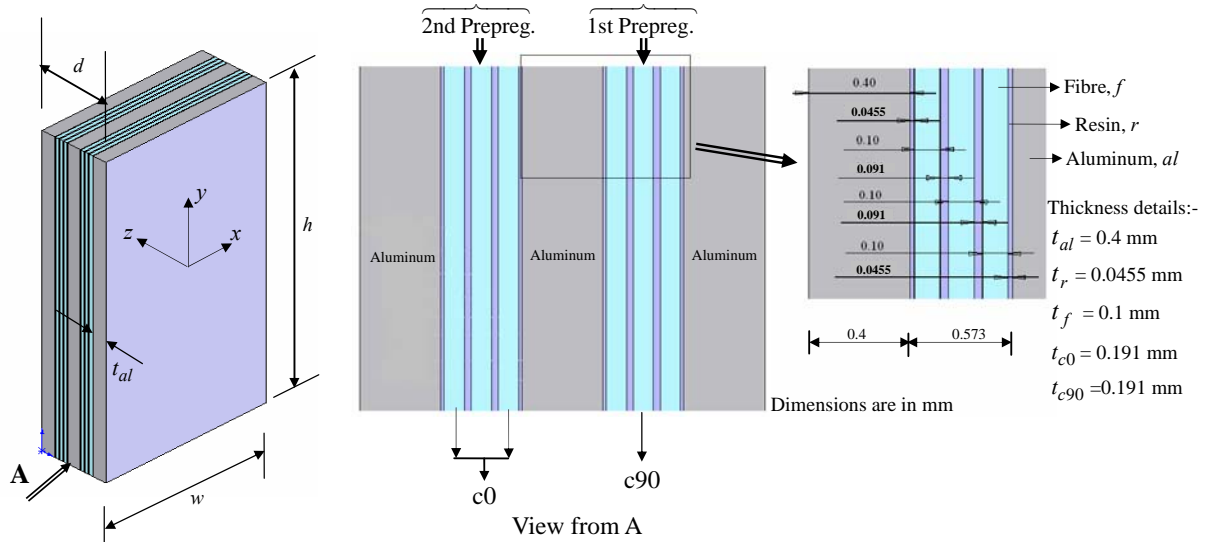


Figure 1. Glare laminate

whereas composite, c90, has fibres laid in x direction i.e. perpendicular to the direction of the applied load. Volume fractions of fibre and resin in each composite layer are 0.522 and 0.478 respectively. The coefficients of thermal expansion of the laminate in longitudinal (y) direction, α_{ll} , and in transverse (x) direction, α_{tt} , are found to be $19.4 \times 10^{-6} \text{ C}^{-1}$ and $19.77 \times 10^{-6} \text{ C}^{-1}$ respectively. Expected dimensions of the laminate were 200 mm (h), 50 mm (w) and 2.346 mm (d). However, minor deviations could not be avoided during fabrication. Important material data are available in Table 1.

Table 1. Material properties

Property	Aluminum 2014-T6 alloy, al (Isotropic)	E-Glass fibre, f (Amorphous)	Epoxy resin, r (Isotropic)
Modulus of elasticity, E (MPa)	72000.0	71000.0	3500.0
Shear modulus, μ (MPa)	27060.0	29710.0	1250.0
Poisson's ratio (ν), % elongation	0.33, 8.0	0.22, 4.8	0.33, 4.0
Yield strength, Y (MPa)	372.0	---	---
Ultimate tensile strength (MPa)	415.0	3450.0	60.0
Coeff. of thermal expansion (α), C^{-1}	23×10^{-6}	5.0×10^{-6}	57.5×10^{-6}
Plane strain fracture toughness (K_{IC}), $\text{MPa}\sqrt{\text{m}}$	14.0-20.0	4.0-5.0	0.5-0.7

3. Theoretical aspects

Stress that develops in un-identical material layers of un-cracked Glare subjected to load differs from the applied stress due to load redistribution caused by elasticity mismatch between the layers. Also, the presence of residual stress, generated in materials during laminate curing due to their varying stiffness and coefficients of thermal expansions, further changes the stress state. The stress-strain constitutive equations and stiffness matrices of the materials in plane stress case (x - y plane) are given as follows:-

i) Aluminum, al

$$\begin{aligned} \sigma_x &= \frac{E_{al}}{(1-\nu_{al}^2)} \{\varepsilon_x + \nu_{al}\varepsilon_y\} \\ \sigma_y &= \frac{E_{al}}{(1-\nu_{al}^2)} \{\nu_{al}\varepsilon_x + \varepsilon_y\} ; \text{ Stiffness matrix, } \{\mathbf{M}\}_{al} = \begin{bmatrix} \frac{E_{al}}{1-\nu_{al}^2} & \frac{E_{al}}{1-\nu_{al}^2}\nu_{al} & 0 \\ \frac{E_{al}}{1-\nu_{al}^2}\nu_{al} & \frac{E_{al}}{1-\nu_{al}^2} & 0 \\ 0 & 0 & \mu_{al} \end{bmatrix} \\ \tau_{xy} &= \mu_{al}\gamma_{xy} \end{aligned}$$

ii) Resin, r

$$\begin{aligned} \sigma_x &= \frac{E_r}{(1-\nu_r^2)} \{\varepsilon_x + \nu_r\varepsilon_y\} \\ \sigma_y &= \frac{E_r}{(1-\nu_r^2)} \{\nu_r\varepsilon_x + \varepsilon_y\} ; \text{ Stiffness matrix, } \{\mathbf{M}\}_r = \begin{bmatrix} \frac{E_r}{1-\nu_r^2} & \frac{E_r}{1-\nu_r^2}\nu_r & 0 \\ \frac{E_r}{1-\nu_r^2}\nu_r & \frac{E_r}{1-\nu_r^2} & 0 \\ 0 & 0 & \mu_r \end{bmatrix} \\ \tau_{xy} &= \mu_r\gamma_{xy} \end{aligned}$$

iii) Fibre, f

$$\begin{aligned} \sigma_x &= \frac{E_f}{(1-\nu_f^2)} \{\varepsilon_x + \nu_f\varepsilon_y\} \\ \sigma_y &= \frac{E_f}{(1-\nu_f^2)} \{\nu_f\varepsilon_x + \varepsilon_y\} ; \text{ Stiffness matrix, } \{\mathbf{M}\}_f = \begin{bmatrix} \frac{E_f}{1-\nu_f^2} & \frac{E_f}{1-\nu_f^2}\nu_f & 0 \\ \frac{E_f}{1-\nu_f^2}\nu_f & \frac{E_f}{1-\nu_f^2} & 0 \\ 0 & 0 & \mu_f \end{bmatrix} \\ \tau_{xy} &= \mu_f\gamma_{xy} \end{aligned}$$

Stiffness matrix of the laminate is obtained from classical theory as follows:-

$$\{\mathbf{M}\}_{lam} = \{\mathbf{M}\}_{al} \times \frac{t_{al} \times 3}{d} + \{\mathbf{M}\}_r \times \frac{t_r \times 12}{d} + \{\mathbf{M}\}_f \times \frac{t_f \times 6}{d}$$

$$\text{For applied stress state over the laminate, } \{\sigma\}_{applied} = \begin{Bmatrix} \sigma_x \\ \sigma_y \\ \tau_{xy} \end{Bmatrix}_{applied},$$

$$\text{Strain in the laminate, } \varepsilon_{lam} = \begin{Bmatrix} \varepsilon_x \\ \varepsilon_y \\ \gamma_{xy} \end{Bmatrix}_{lam} = \{\mathbf{M}\}_{lam}^{-1} \sigma_{applied}$$

Residual strain (rs) in material layers is written as:-

$$\text{Aluminum, } \{\varepsilon\}_{al,rs} = \begin{bmatrix} \left\{ \begin{matrix} \alpha_x \\ \alpha_y \\ 0 \end{matrix} \right\}_{al} - \left\{ \begin{matrix} \alpha_{tl} \\ \alpha_{ll} \\ 0 \end{matrix} \right\} \end{bmatrix} \times (T_{curing} - T_{ambient})$$

$$\text{Resin, } \{\varepsilon\}_{r,rs} = \begin{bmatrix} \left\{ \begin{matrix} \alpha_x \\ \alpha_y \\ 0 \end{matrix} \right\}_r - \left\{ \begin{matrix} \alpha_{tl} \\ \alpha_{ll} \\ 0 \end{matrix} \right\} \end{bmatrix} \times (T_{curing} - T_{ambient})$$

$$\text{Fibre, } \{\varepsilon\}_{f,rs} = \begin{bmatrix} \left\{ \begin{matrix} \alpha_x \\ \alpha_y \\ 0 \end{matrix} \right\}_f - \left\{ \begin{matrix} \alpha_{tl} \\ \alpha_{ll} \\ 0 \end{matrix} \right\} \end{bmatrix} \times (T_{curing} - T_{ambient})$$

Residual stress in aluminum = $\{\mathbf{M}\}_{al} \times [\{\varepsilon\}_{al,rs}]$; Residual stress in resin = $\{\mathbf{M}\}_r \times [\{\varepsilon\}_{r,rs}]$; Residual stress in

$$\text{fibre} = \{\mathbf{M}\}_f \times \{\{\varepsilon\}_{f,rs}\}$$

Stress developing in material layers (Induced stress), $\{\sigma\}_{induced} = \begin{Bmatrix} \sigma_x \\ \sigma_y \\ \tau_{xy} \end{Bmatrix}_{induced}$, is determined as follows:-

$$\{\sigma\}_{induced,al} = \{\mathbf{M}\}_{al} \times [\varepsilon_{lam} + \{\varepsilon\}_{al,rs}]; \{\sigma\}_{induced,r} = \{\mathbf{M}\}_r \times [\varepsilon_{lam} + \{\varepsilon\}_{r,rs}]; \{\sigma\}_{induced,f} = \{\mathbf{M}\}_f \times [\varepsilon_{lam} + \{\varepsilon\}_{f,rs}]$$

In the case of cracked Glare, stress state around cracked aluminum and affected fibre zone differs from the induced stress due to the presence of crack and onset of the process of fibre bridging. These effects are assessed numerically in Section 5.

Plane stress fracture toughness or induced stress intensity parameter of Glare, at fracture (fr), containing cracks of length, c , in aluminum layers is obtained from the following expression pertaining to Linear Elastic Fracture Mechanics (LEFM)

$$K_{C,lam} = (\sigma_{y,induced,al})_{fr} \times \sqrt{\pi c} \times CF \quad (1)$$

where configuration factor, CF , for an edge crack is empirically given by $CF = \left[1.12 - 0.23 \frac{c}{w} + 10.55 \left(\frac{c}{w} \right)^2 - 21.72 \left(\frac{c}{w} \right)^3 + 30.39 \left(\frac{c}{w} \right)^4 \right]$ and, w , is the width of the laminate. For cracked plain aluminum alloy specimen, the expression takes the form, $K_{C,al} = (\sigma_{y,applied})_{fr} \times \sqrt{\pi c} \times CF$, term $(\sigma_{y,induced,al})_{fr}$ used in the laminate being replaced by $(\sigma_{y,applied})_{fr}$ since load redistribution does not take place in plain specimen. In the case of a thin plain specimen, plane strain fracture toughness, $K_{IC,al}$, is estimated from plane stress toughness value, $K_{C,al}$, by the following expression [3]

$$K_{C,al} = K_{IC,al} \left[1 + \frac{1.4}{p^2} \left(\frac{K_{IC,al}}{Y_{al}} \right)^4 \right]^{1/2} \quad (2)$$

where p is the thickness of the specimen. Knowing $K_{IC,al}$, plane stress toughness of hypothetical plain aluminum alloy specimen, $K_{C,al}^d$, with higher thickness, d , equal to that of Glare laminate, is again obtained from Eq. (2). The following condition holds good in Glare at fracture

$$K_{C,lam} = K_{tip} + K_{br} \text{ or } K_{C,lam} = K_{C,al}^d + K_{br} \text{ since } K_{tip} = K_{C,al}^d \quad (3)$$

where K_{tip} is the crack tip stress intensity parameter and K_{br} is the bridging stress intensity parameter. Fulfillment of the conditions, $t_{al} < 2.5 \left(\frac{K_{IC,al}}{Y_{al}} \right)^2$ and $p < 2.5 \left(\frac{K_{IC,al}}{Y_{al}} \right)^2$, supports plane stress conditions in cracked aluminum of Glare and of plain specimen respectively.

4. Experimental work

Starter notches were machined across the interfaces of all material layers at the edges of Glare laminates. Mode I cracks, nucleated at notch tips by fatigue cycles, were made to grow up to

lengths, c , of 5 mm, 7 mm, 9.5 mm, 14 mm and 20 mm in laminates numbered 1 to 5 respectively. Refer Figure 2a). As expected, the cracks developed in all soft aluminum layers and not in stronger fibres of prepreps. No interfacial crack growth (Delamination) was observed at aluminum fibre interfaces. Each cracked laminate was then subjected to load-extension test in a hydraulic test rig to measure the load line stress applied over it at fracture, $(\sigma_{y,applied})_{fr}$. Refer Figure 3 for the test arrangement. At fracture, aluminum layers failed first by critical crack growth followed by stretching of fibre layers till the laminate separated. $(\sigma_{y,applied})_{fr}$ values varied in the laminates due to different crack sizes in them. As explained in Section 3, induced stress in aluminum layers at fracture, $(\sigma_{y,induced,al})_{fr}$, was different from $(\sigma_{y,applied})_{fr}$. The values are provided in Table 2. Refer Figure 2b). Five cracked specimens of plain aerospace aluminum 2014-T6 alloy, also numbered 1 to 5, with small thickness, p , but same crack sizes and other dimensions similar to the laminates, were also tested for fracture. For same crack length, $(\sigma_{y,applied})_{fr}$ values of plain aluminum alloy specimens were found to be greater than that of the laminates due to smaller thickness of the former. Thickness effects were however nullified by obtaining $K_{C,al}^d$. Sample load-extension curves of laminate and of plain aluminum specimen at 20 mm crack length are displayed in Figure 4. All the curves, including those at other crack lengths also, were mostly found to be linear even near fracture loads, because of low ductility of aluminum alloy. The principles of LEFM were therefore valid and the use of parameter K for fracture characterization was justified.

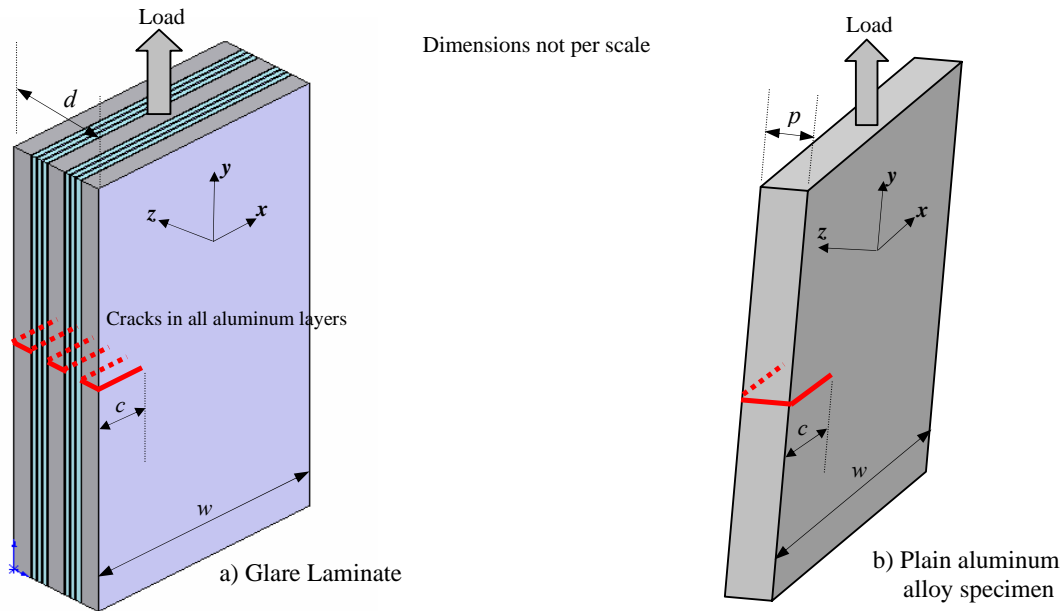


Figure 2. Crack configuration in Glare laminate and in plain aluminum alloy specimen

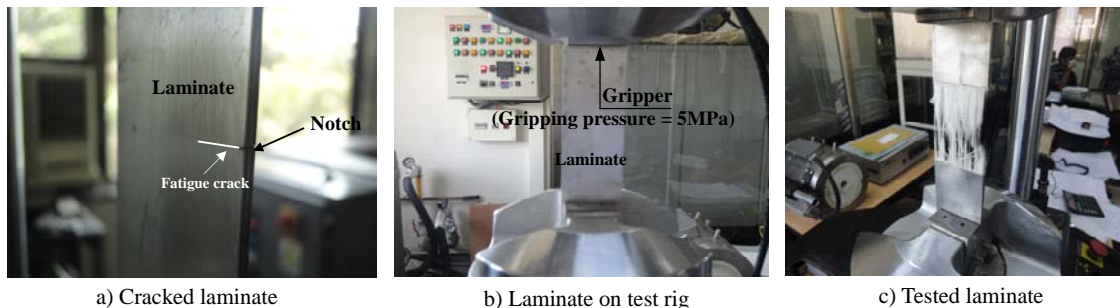
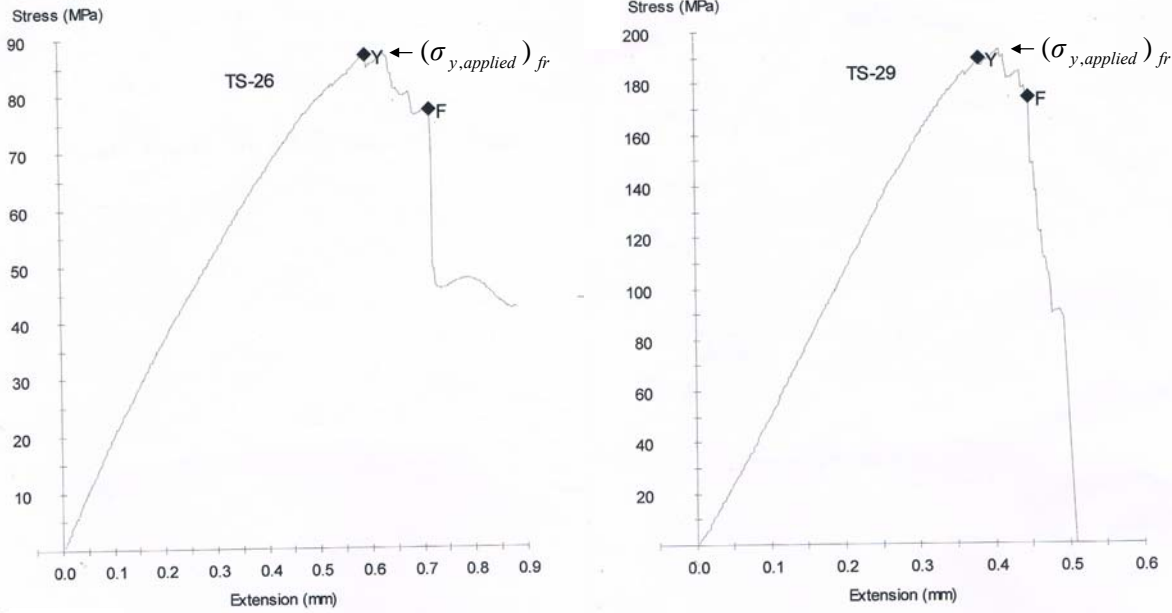


Figure 3. Fracture test arrangement



a) Glare Laminate

b) Plain aluminum alloy specimen

Figure 4. Sample load-extension plots of Glare laminate and of plain aluminum alloy specimen with 20 mm long cracks

Table 2. Critical stress and fracture toughness of Glare laminates and of plain aluminum alloy specimens

Glare laminates								
Laminate No.	d (mm), t_{al} (mm)	c (mm)	w (mm)	CF	$(\sigma_{y,applied})_{fr}$ (MPa)	$(\sigma_{y,induced,al})_{fr}$ (MPa)	$K_{C,lam}$ (MPa \sqrt{m})	$K_{C,al}^d = K_{tip}$ (MPa \sqrt{m})
1	2.39, 0.53	5.0	50.0	1.183	120.0	204.36	30.32	18.40
2	2.30, 0.5	7.0	49.6	1.248	150.0	243.27	45.05	18.67
3	2.50, 0.5	9.5	51.0	1.34	210.0	321.16	74.33	18.10
4	2.20, 0.4	14.0	50.3	1.587	120.0	204.36	68.04	19.00
5	2.50, 0.4	20.0	50.7	2.07	90.0	165.36	85.96	18.10
Refer Section 3, Induced stress value in fibre at fracture is given below: - (+ve is tensile and -ve is compressive)								
Laminate No. 1: $(\sigma_{y,induced,f})_{fr} = -21.92$ MPa, Laminate No. 2: $(\sigma_{y,induced,f})_{fr} = +15.36$ MPa								
Laminate No. 3: $(\sigma_{y,induced,f})_{fr} = +89.91$ MPa, Laminate No. 4: $(\sigma_{y,induced,f})_{fr} = -21.92$ MPa								
Laminate No. 5: $(\sigma_{y,induced,f})_{fr} = -59.2$ MPa								
Plain aluminum alloy specimens								
Specimen No.	p (mm)	c (mm)	w (mm)	CF	$(\sigma_{y,applied})_{fr}$ (MPa)	$K_{C,al}$ (MPa \sqrt{m})	$K_{IC,al}$ (MPa \sqrt{m})	
1	0.66	5.0	50.20	1.182	280	41.53	14.48	
2	0.65	7.0	50.45	1.244	240	44.30	14.70	
3	0.86	9.5	50.50	1.343	75	17.41	11.06	
4	0.60	14.0	50.45	1.580	210	69.80	16.81	
5	0.36	20.0	50.36	2.088	190	99.47	16.05	
Average $K_{IC,al} = 14.62$ MPa \sqrt{m}								

5. Numerical analysis

Refer Figure 5a). 3D finite element models of all cracked Glare laminates without delaminations were created with 8 noded, solid 185 elements in aluminum and 8 noded, layered solid shell 190 elements in fibre and resin layers. Half of the laminates were only modeled due to symmetry. The bottom nodes representing cracks in all aluminum and resin layers were unconstrained while the nodes of un-cracked fibre layers were constrained in y direction ($v = 0$) as shown in Figure 5b). Stress-strain data of materials, available in Figure 6, were used in the material models of the software. Fracture stress values, $(\sigma_{y,applied})_{fr}$, taken from Table 2, were applied at the top edges of the laminates. Residual stress developing in materials during laminate curing at 160 deg. C, whose values were obtained using $T_{curing} = 160$ deg. C and $T_{ambient} = 30$ deg. C in Section 3, were introduced over nodes in x and y directions. The residual stress was same in all the laminates. Their values are given below (+ve is tensile and -ve is compressive):-

- i) Aluminum = 46.17 MPa (+ve) in x dir., 48.36 MPa (+ve) in y dir.
- ii) Resin = 25.59 MPa (+ve) in x dir., 25.73 MPa (+ve) in y dir.
- iii) Fibre = 173.92 MPa (-ve) in x dir., 171.02 MPa (-ve) in y dir.

Crack energy release rate can be represented by J integral in LEFM. J in x - y plane over cyclic path, P , [4] is defined by the summation of different terms at nodes on the path as follows:-

$$J = \int_P (W_e dy - T_x \frac{\partial u}{\partial x} ds - T_y \frac{\partial v}{\partial x} ds) \quad (4)$$

where W_e is the strain energy density, $T_x = \sigma_x n_x + \tau_{xy} n_y$ and $T_y = \sigma_y n_y + \tau_{xy} n_x$ are traction terms with n_x and n_y in the expressions representing unit vectors in x and y directions and u and v are displacements in stated directions. To estimate the shielding effect at the crack tips, values of J integral, J_{tip} , were found over several paths around crack tip, as shown in Figure 5b), which were then averaged to obtain the final value. Laminates without cracks were also modeled under $(\sigma_{y,applied})_{fr}$ and residual stress stated above. Their constraints are shown in Figure 5c). Since J integral value does not critically depend upon the mesh type, a simpler mesh scheme was adopted in place of square root singularity mesh type around the crack tips.

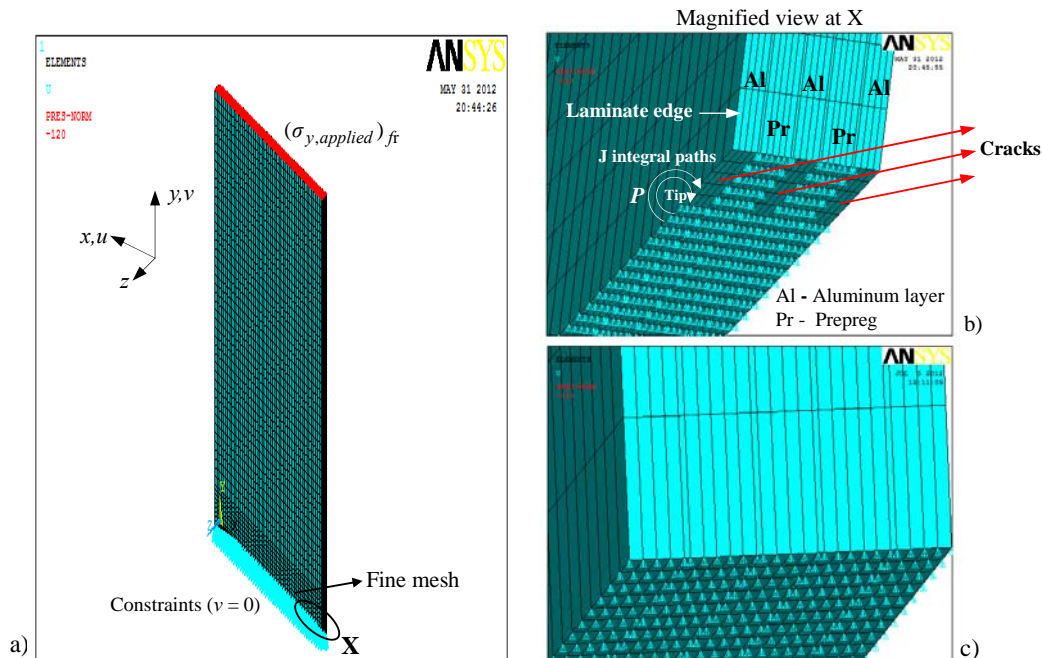


Figure 5. a) Finite element model of Glare b) Constraints in cracked Glare
c) Constraints in un-cracked Glare

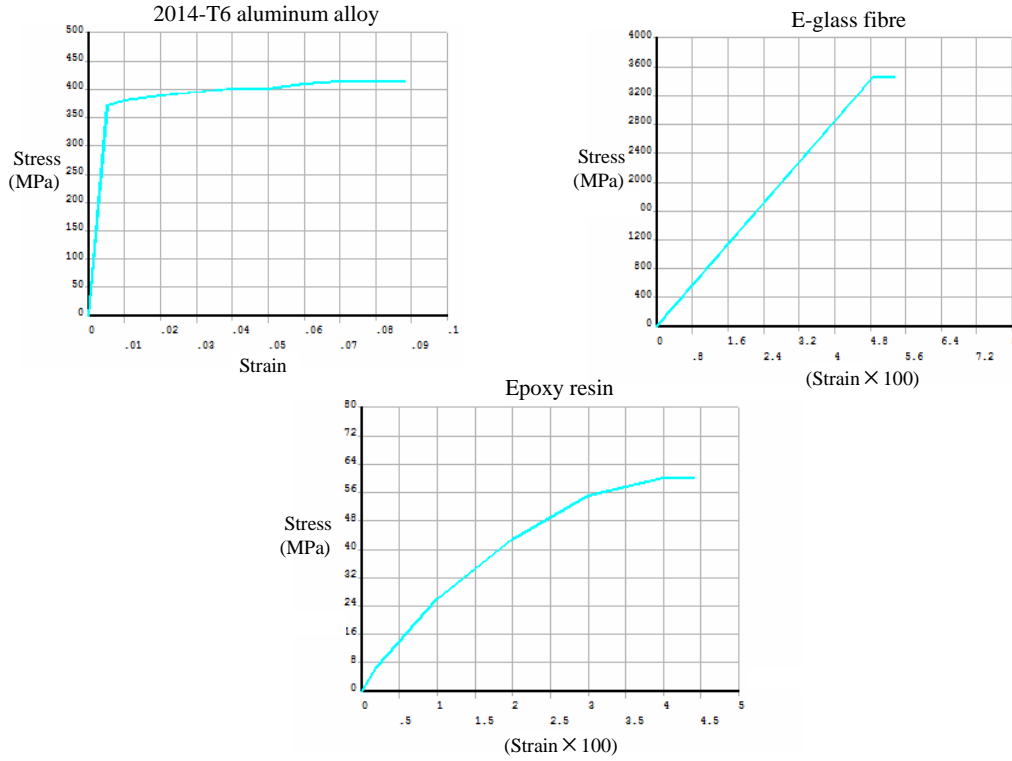


Figure 6. Stress-strain plots of materials

K_{tip} values were finally obtained from J_{tip} by LEM relation in plane stress condition, $K_{tip} = \sqrt{E_{al} J_{tip}}$. They are presented in Table 3.

Table 3. Numerical values of stress intensity parameter at crack tips in Glare laminates

Laminate No.	J_{tip} (N/mm)	K_{tip} (MPa \sqrt{m})
1	1.093	8.85
2	1.947	11.84
3	2.899	14.44
4	1.718	11.123
5	0.799	7.58

6. Observations

Refer Figure 7a) and 7b). Numerical values of, load line, induced stress in aluminum layer and in fibre layer, $(\sigma_{y,induced,al})_{fr}$ and $(\sigma_{y,induced,f})_{fr}$ respectively, of un-cracked Glare, are close to the values available in Table 2 that validates the finite element model. Sample load line stress in aluminum layer and in fibre layer, $(\sigma_{y,total,al})_{fr}$ and $(\sigma_{y,total,f})_{fr}$, of cracked Glare containing 5 mm crack are provided in Figure 7c) and 7d). Since no yielding is observed at the crack tip, LEM regime is numerically confirmed. In addition, the values of $\frac{(\sigma_{y,total,al})_{fr}}{Y_{al}}$ are less than 0.5 that further support LEM conditions in cracked aluminum.

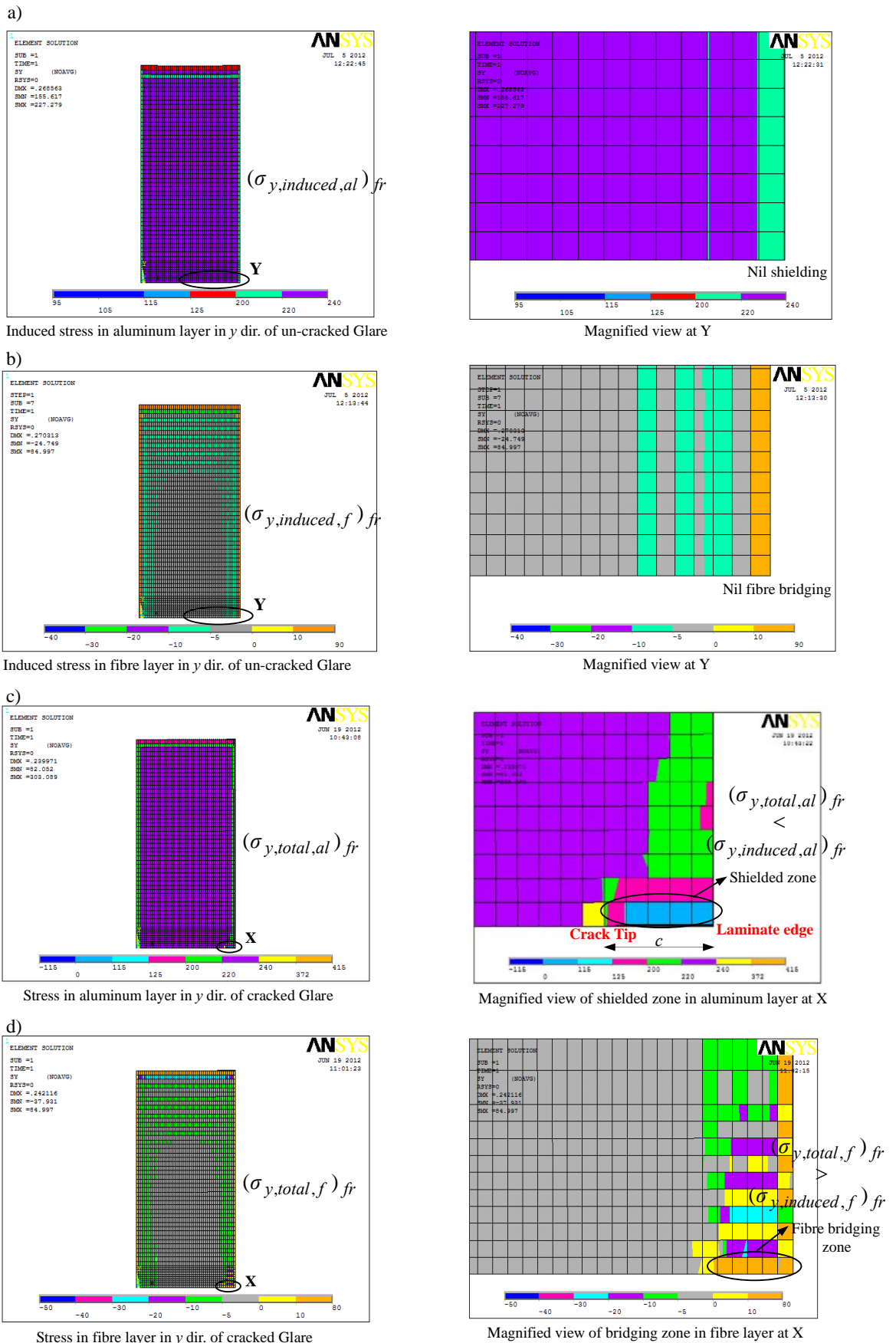


Figure 7. Load line stress plots in un-cracked and cracked Glare laminate with 5 mm crack

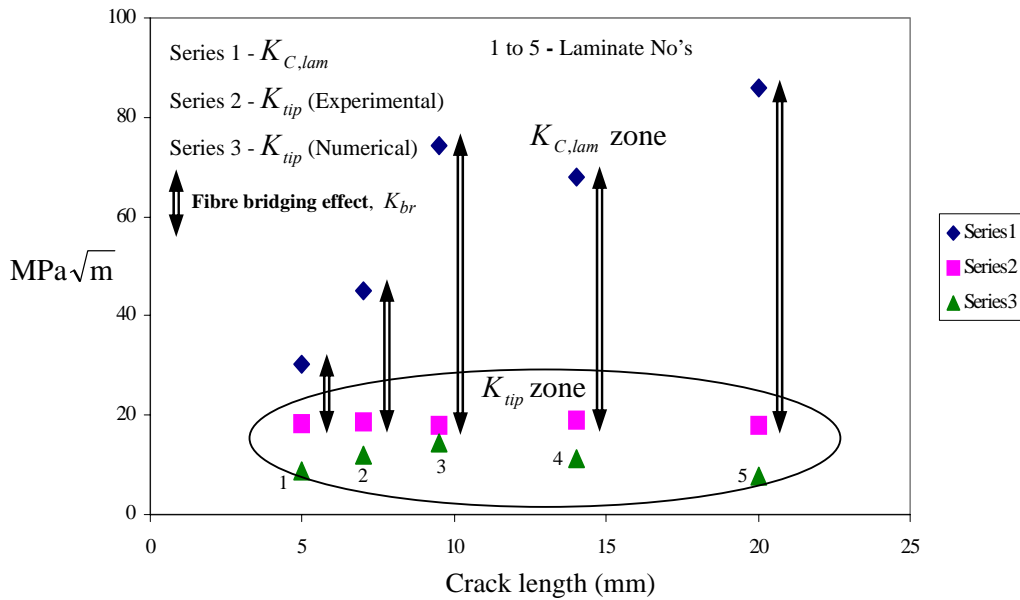


Figure 8. Comparison between experimental and numerical estimations of fibre bridging

Fulfillment of the condition, $(\sigma_{y,total,f})_{fr} > (\sigma_{y,induced,f})_{fr}$, in bridging zone of fibre layer convincingly confirms load transfer towards fibre. Also, $(\sigma_{y,total,al})_{fr} \ll (\sigma_{y,induced,al})_{fr}$, around cracked area of aluminum hints at the shielding effect. Although the presence of crack, as a free surface, in itself dips the load line stress field in shielded area of aluminum, the magnitude of $\{(\sigma_{y,total,al})_{fr} - (\sigma_{y,induced,al})_{fr}\}$ is found to be high enough to include both the compressive effects i.e. due to the crack and due to shielding by fibre bridging. Similar trends are observed in laminates with cracks of other sizes as well. Again from the experimental results in Table 2, the finding, $K_{C,lam} > K_{tip}$ or $K_{C,lam} > K_{C,al}^d$, adequately proves crack tip shielding and enhanced fracture toughness of the laminates vis-à-vis corresponding plain aerospace aluminum alloy specimens. Experimental and numerical results of K_{tip} are compared in Figure 8. They are close to each other. The error is attributed to slight difference between theoretical and experimental values of residual stress in aluminum layer of the laminate. The experimental values are lower than the theoretical ones. Fibre bridging effect, K_{br} , is quantified by $\{K_{C,lam} - K_{tip}\}$. The effect, in general, is found to increase with increase in crack size in aluminum layers. Absence of delaminations intensifies the effect.

Acknowledgements

The author is grateful to Science and Engineering Research Council, Department of Science and Technology, The Government of India for funding the project. Support received from the School of Mechanical and Building Sciences, VIT University, Vellore, India during the course of this work is acknowledged.

References

- [1] Y.J. Guo, X.R. Wu, Bridging stress distribution in center-cracked fibre reinforced metal laminate: Modeling and Experiment. Eng Fra Mech, 63 (1999) 147-163.
- [2] R.C. Alderliesten, Analytical prediction model for fatigue crack propagation and delamination growth in Glare, Int J Fat, 29 (2007) 628-646.
- [3] G.R. Irwin, NRL Report 6598, 1967.
- [4] J.R. Rice, A path independent integral and approximate analysis of strain concentration by notches and cracks. J App Mech, 35 (1968) 379-386.